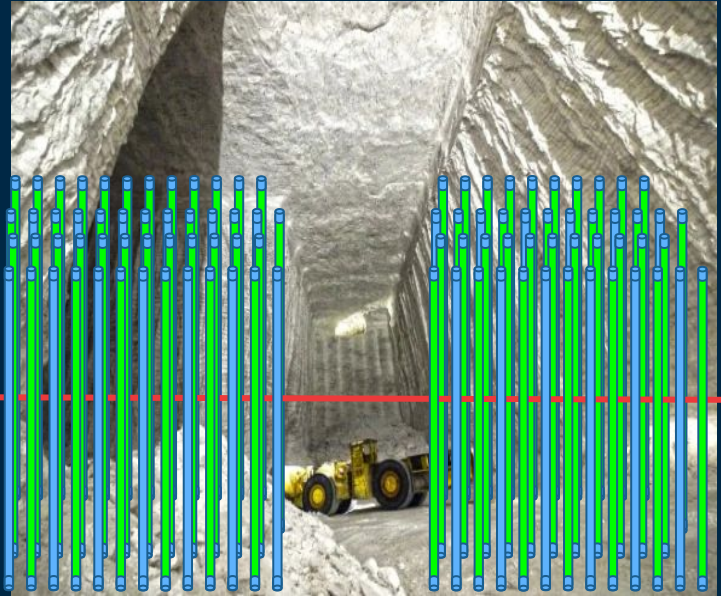


Directional Response of Several Geometries for Reactor-Neutrino Detectors

Presenter: Max Asa Albert Dornfest (University of Hawai'i at Manoa)
Co-authors: Brian C. Crow, Mark J. Duvall, Viacheslav A. Li, Jeffrey G. Yopez
Principle Investigator: Prof. John G. Learned
Conference: Applied Antineutrino Physics (AAP) 2024, RWTH Aachen, Germany



<https://decommissioningcollaborative.org/perry/page/2/>



LLNL-PRES-871056. This work was performed under the auspices of the U.S. Department of Energy by Lawrence Livermore National Laboratory under Contract DE-AC52-07NA27344.
https://www.canadianmanufacturing.com/wp-content/uploads/2016/07/bergbau_KS_sait_mine.jpg



Outline of talk – Part 1

Directional Response of Several Geometries for Reactor-Neutrino Detectors [arXiv:2402.01636](https://arxiv.org/abs/2402.01636)

- Accepted by Phys. Rev. Applied, 20th September 2024
- Introduction to directionality from inverse beta decay (IBD)
- Monolithic Detectors - Chooz and Double Chooz
- 2D - SANDD and Prospect
- 2D Checkerboard
- 3D - NuLat 5
- 3D Checkerboard

Results

- Radar Plot - Directionality
- Primary results - Angular Uncertainty

Outline of talk – Part 2

- Relating back to past AAP conferences

FROST – Forest of Scintillating Tubes

- FROST in 1-minute
- FROST in lab
- FROST-TEA

Early Preliminary and Future Work

- Simulations for small modular reactors (SMRs)
 - Analytical
 - Max's dummy variable model (one hot encoding)

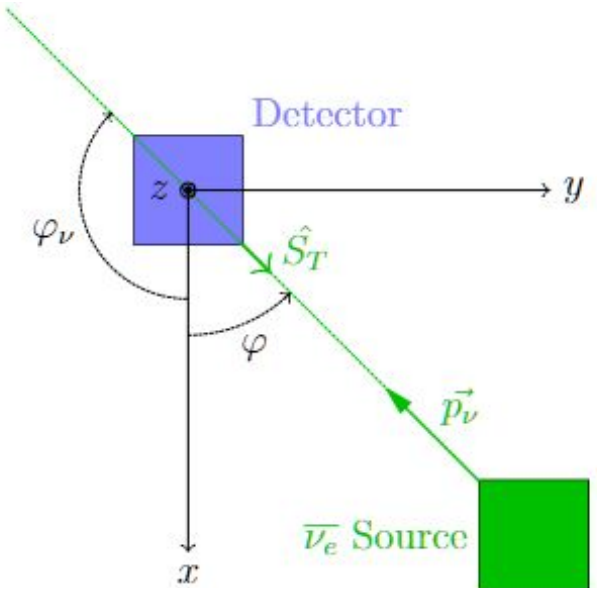
Concluding Remarks and Acknowledgements

Directionality

Introduction to directionality from IBD



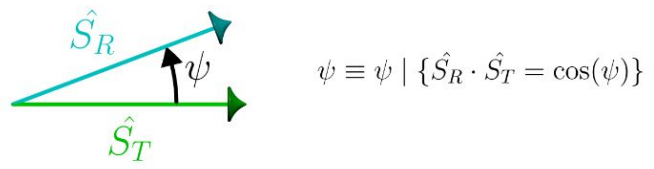
Directionality From Inverse Beta Decay - Definitions



$$\varphi \equiv \varphi_{source} = \varphi_{\nu} \pm 180^{\circ}, \quad (1)$$

$$\varphi_{\nu} = \arctan\left(\frac{p_{\perp}}{p_{\parallel}}\right) = \arctan\left(\frac{\Delta y}{\Delta x}\right) \quad (2)$$

(a) Definition of Reconstruction Vector \vec{S}_R



$$\psi \equiv \psi \mid \{ \hat{S}_R \cdot \hat{S}_T = \cos(\psi) \}$$

(b) Definition of ψ as the Angle Between the True (\hat{S}_T) and Reconstructed (\hat{S}_R) Source Directions

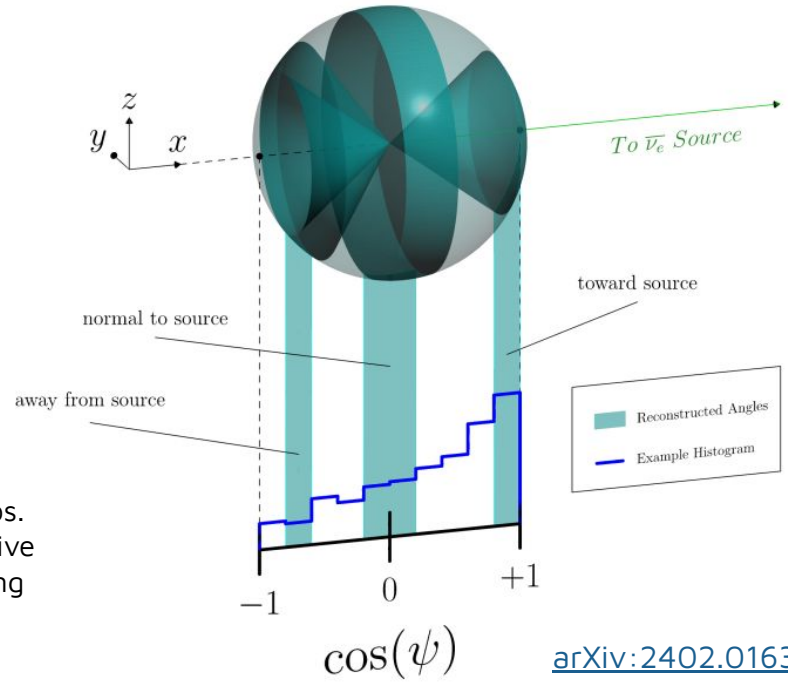


Fig. (left) Illustrating directionality as applied to a detector attempting to reconstruct the direction \hat{S}_T (\hat{S}_{True}) to the source of the incoming antineutrinos. In the case shown, the source is assumed to be location on the horizon relative to the detector (i.e. $z_{detector} = z_{source}$), so this problem reduces to reconstructing the azimuthal angle φ which can be found as given in equations (1) and (2).

Fig. (right) Physical meaning of $\cos\psi$ distributions.

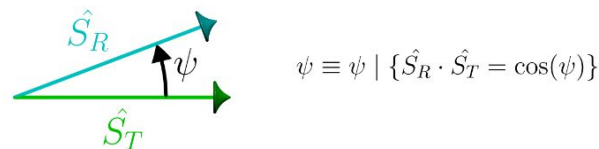
Directionality From Inverse Beta Decay - Definitions

Fig. (right) **Physical meaning of $\cos \psi$ distributions**, illustrated here as it applies to the 3D experiments.

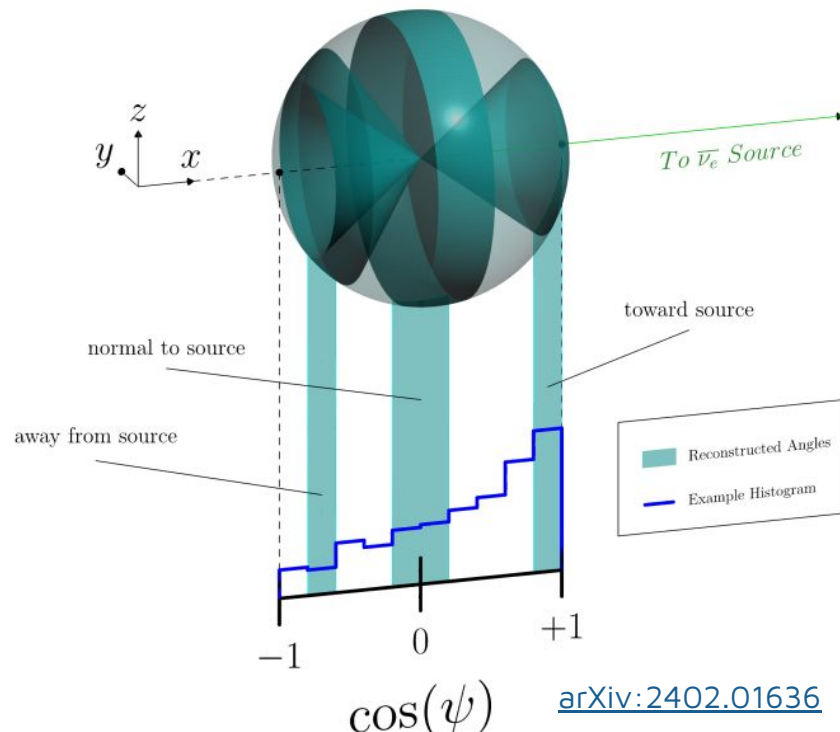
Events in the leftmost shaded region (i.e., the second bin from the left in the example histogram) **correspond to reconstructed angles falling within the solid angle between the two cones** defined by $\cos \psi = -0.8$ and $\cos \psi = -0.6$, or $\psi \approx 143^\circ$ and $\psi \approx 127^\circ$

The 2D analogue is the projection of this diagram onto the x-y plane.

(a) Definition of Reconstruction Vector \vec{S}_R



(b) Definition of ψ as the Angle Between the True (\hat{S}_T) and Reconstructed (\hat{S}_R) Source Directions



Directionality From Inverse Beta Decay - Statistics and Analytical Limit

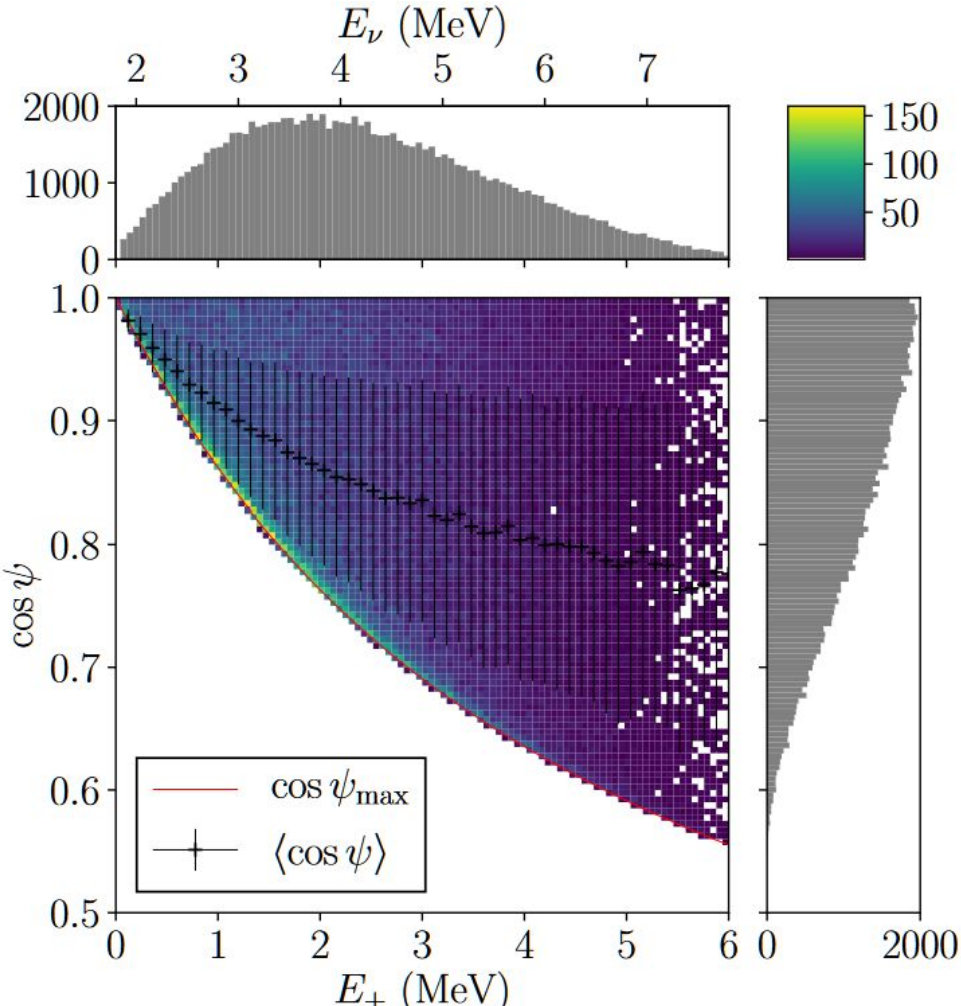
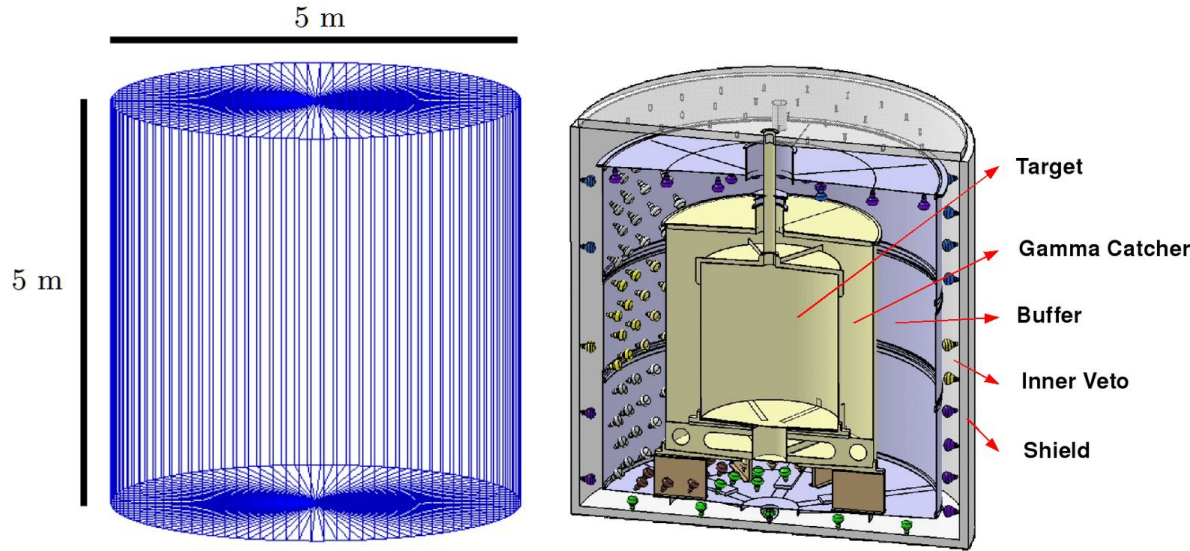


Figure: Distribution of positron kinetic energy E_+ and \cos of neutron scattering angle (ψ) relative to the incoming antineutrino, simulated via RAT-PAC.

- Based on simulating 100,000 IBD positron-neutron pairs.
- **Red line** along LHS boundary shows constraint from analytical maximum, when the angle approaches the **maximum allowed angle**.
- The binning in both axes, $\cos \psi$ and positron energy E_+ , is 100; the projections are shown in gray in the inset 1D histograms.

Monolithic / Single Volume – Double Chooz



Double Chooz chosen as a basis for comparison with Erica Caden’s “Studying Neutrino Directionality with Double Chooz”.

In Chooz and Double Chooz, all of the target material is arranged in a single, central, volume.

We will hereafter refer to this basic design as the “monolithic” type detector.

Figure(s) above: Geometry of one simulated DC model without PMTs (left). General design diagram of DC (right).

Segmented - 2D - PROSPECT and SANDD

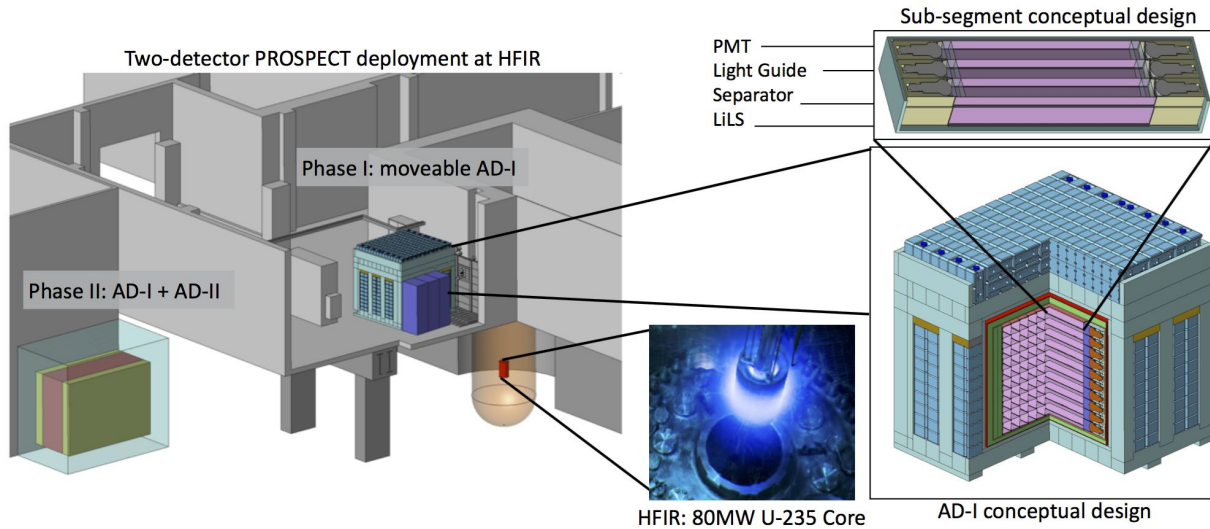


Fig. Below: Central Module of SANDD (Segmented AntiNeutrino Directional Detector). SANDD consists of (a) sixty-four ${}^6\text{Li}$ -loaded plastic-scintillator rods, attached to the SiPM arrays (b) cross section bars wrapped in PTFE tape attached to 1" PMTs.

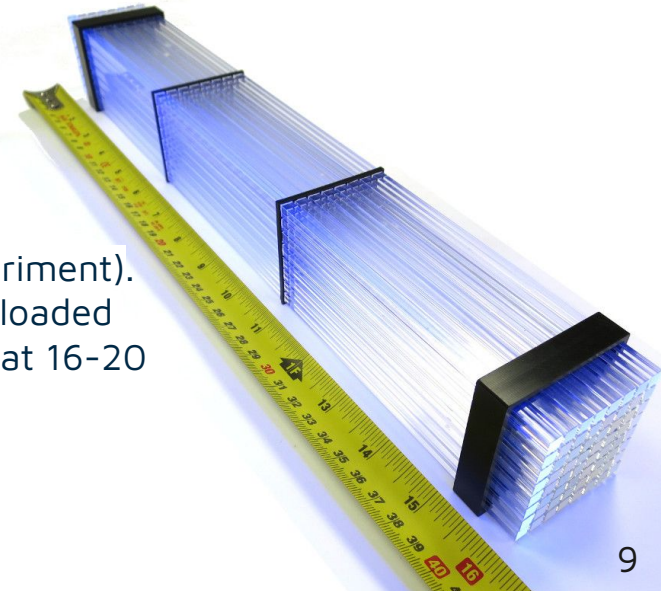


Fig. Above: PROSPECT (Precision Reactor Oscillation and SPECTrum Experiment). PROSPECT-I was a acrylic shell containing ~four tons of liquid scintillator loaded with ${}^6\text{Li}$. Phase II adds a 10-ton active mass antineutrino detector (AD-II) at 16-20 meters from the reactor core.



Photo from <https://prospect.yale.edu/science>

Segmented - 2D Checkerboard

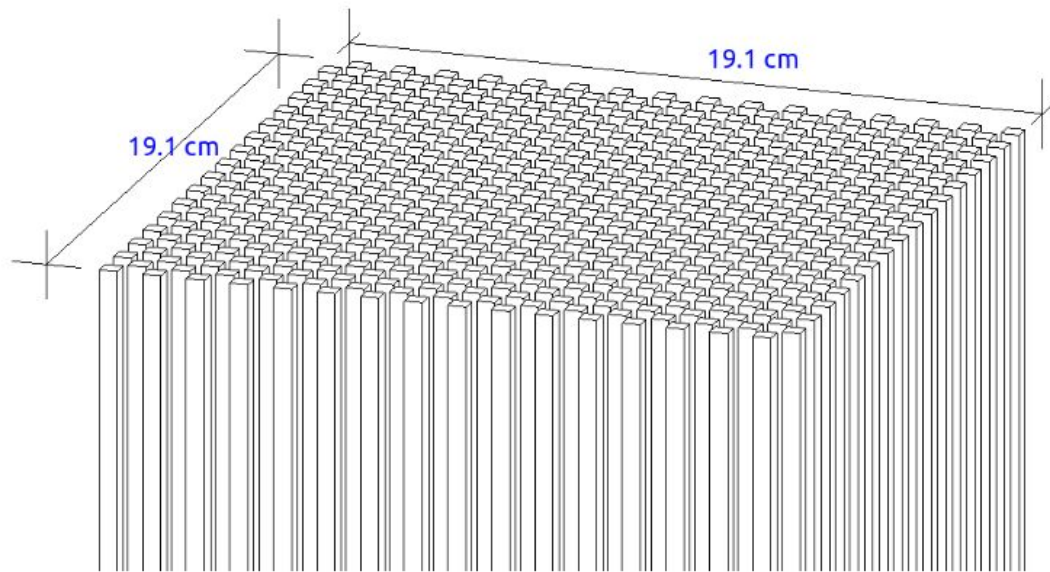
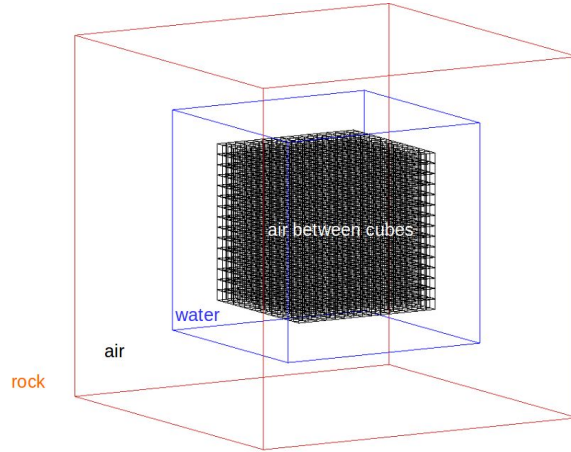


Fig. 2D Checkerboard geometry as used in simulation work.

Segmented - 3D - NuLat (Neutrino Lattice)



A key limitation of the monolithic approach is a spatial resolution which is typically considerably larger than the neutron-displacement distance.

The goal: a measurement of the neutron's displacement.

- This depends on determining the brightest cube.
- 2x PMT signal on each axis enabling 3D reconstruction.
- In our paper we studied NuLat 5. Cubes have 5cm side lengths each with 1cm airgaps. ([NuLat: A new type of Neutrino Detector for Sterile Neutrino Search at Nuclear Reactors and Nuclear Nonproliferation Application](#))

Fig. Above: NuLat 5 using LEDs to show total internal reflection in Raghavan Optical Lattice (left). Geometry of NuLat and environment simulated (right).

Segmented - 3D Checkerboard

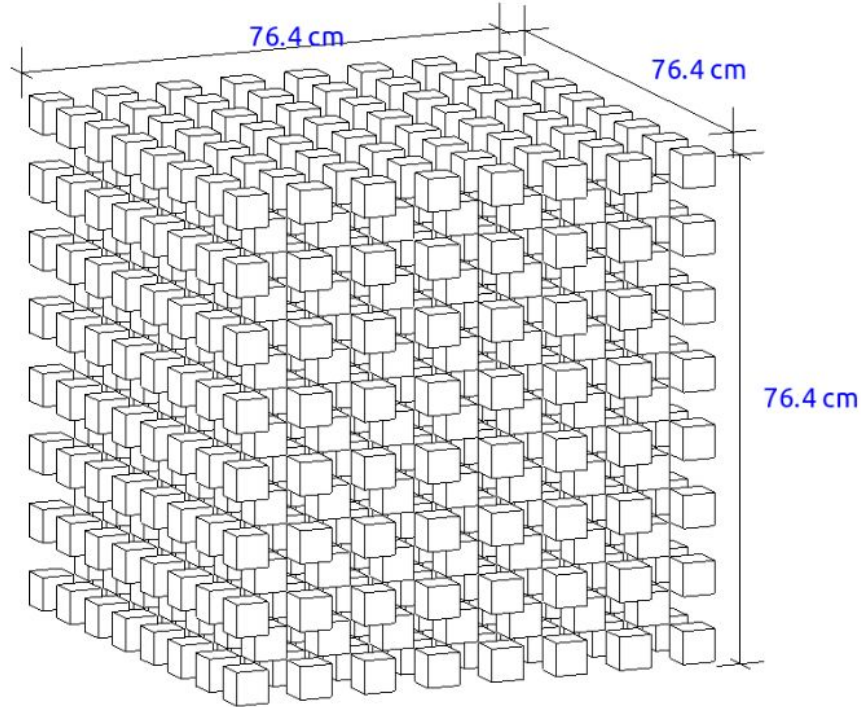


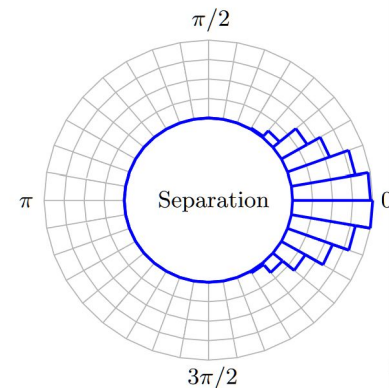
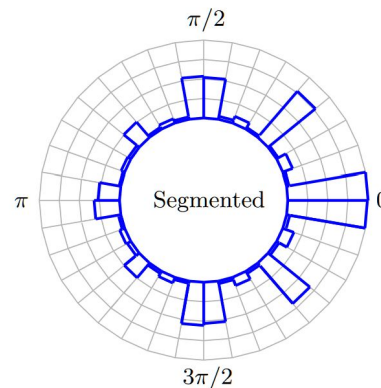
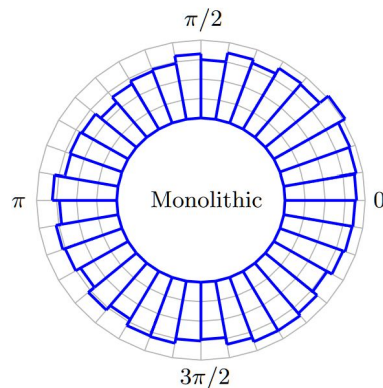
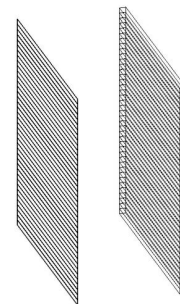
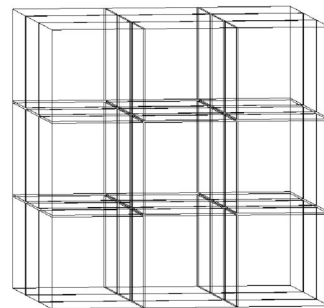
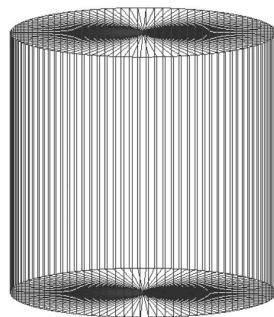
Fig. 3D Checkerboard geometry as used in simulation work.

Results - Radar Plot

Figure(s) (right): Geometry and distributions of the azimuthal angle φ for three selected geometries:

monolithic (Double Chooz),
segmented (NuLat 5), and
separation (SANTA, Segmented AntiNeutrino Tomography Apparatus).

The bin width is 10° ; the inner circle on each histogram corresponds to 0 events and the outer circle is normalized to the max number of events per bin.



Primary Result - Angular Uncertainty

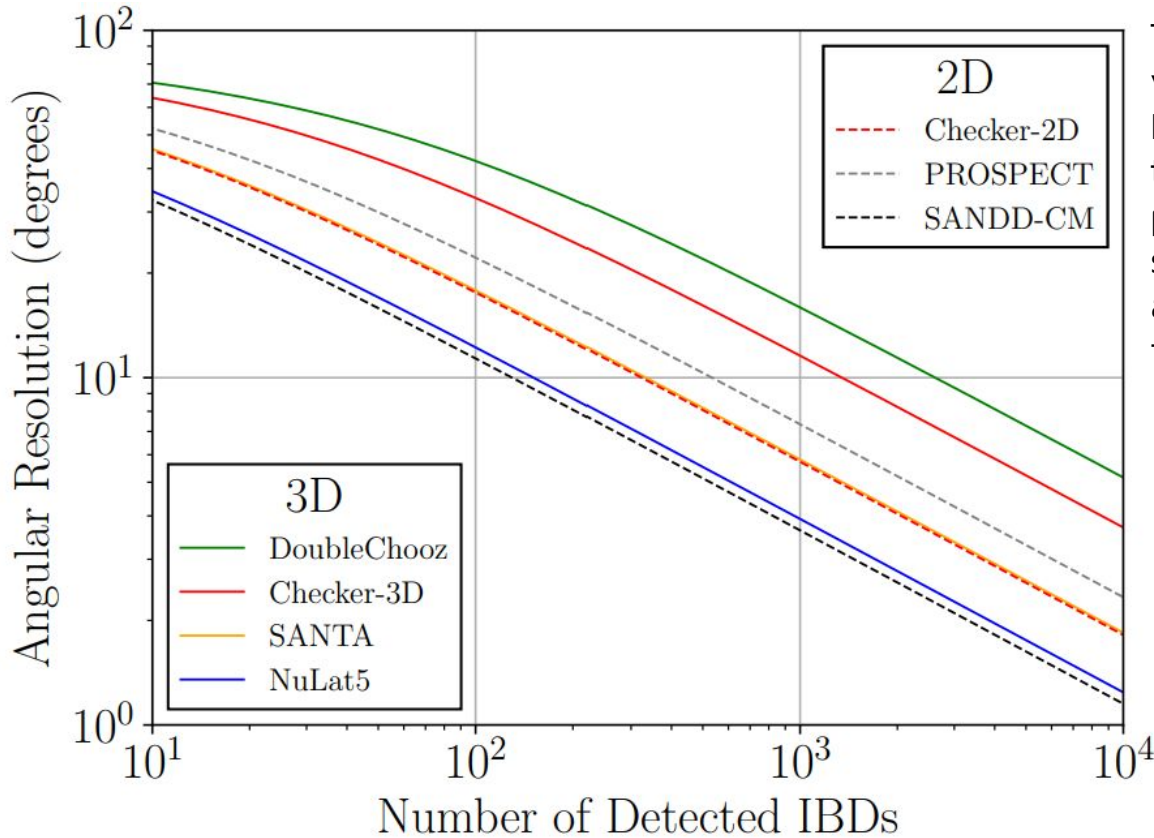


Fig. Angular uncertainty $\Delta\varphi$ as a function of detected IBD events for various detector designs (2D detectors indicated by a dashed line; 3D — by a solid line).

The calculation is based on using the values for the mean position resolution P and the mean distance d_n (between the prompt and delayed events) presented in our results Table for the simulated detector geometries, as well as taking into account the packing factor Π in the following equation:

$$[\Delta\varphi]_{1\sigma} = \arctan\left(\frac{P/d_n}{\sqrt{N\Pi}}\right)$$

Where $[\Delta\varphi]_{1\sigma}$ is 1σ angular uncertainty on the \vec{v}_e reconstructed direction, P is the mean position, d_n is the mean distance between the prompt and delayed events, and N is the number of IBD events.

Relating to past AAP conferences

AAP 2004

Neutrinos and Arms Control Workshop February
2004, University of Hawaii

AAP 2018

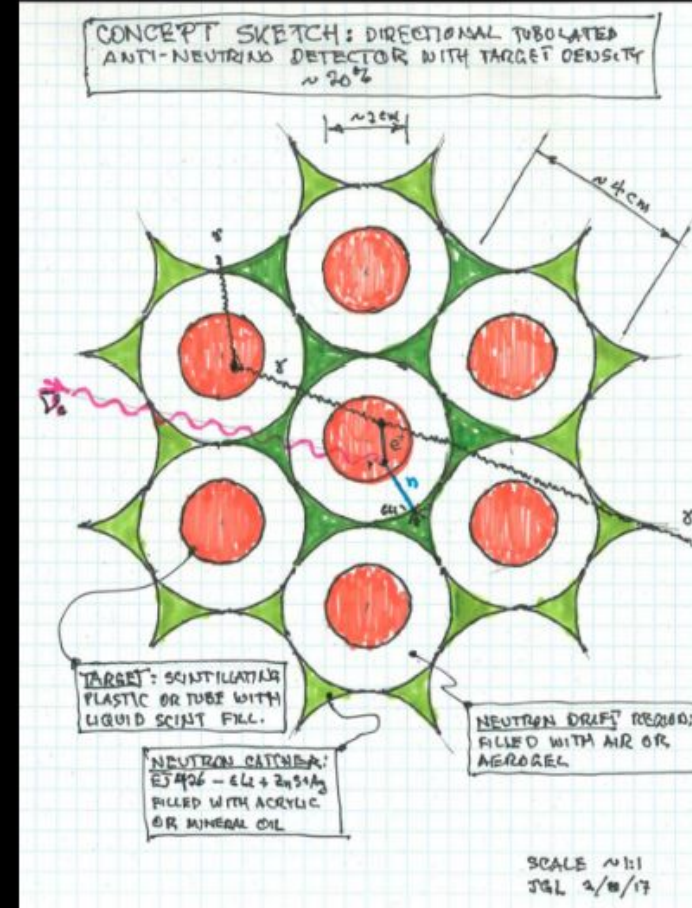
Antineutrino Directionality R&D - Daine Danielson

<https://www.phys.hawaii.edu/aap/>




Antineutrino Directionality R&D by Daine Danielson, AAP 2018

- New concept by John Learned
- Aims to combine strengths of SANTA with those of segmented detectors
- Potential for a large target volume
- 180° angular acceptance
- **Needs further study!**



FROST: Forest Of Scintillating Tubes

The background features several vertical white lines of varying lengths. Interspersed among these lines are small squares in various colors: light blue, orange, pink, and cyan. Some squares are solid, while others are hollow. The overall aesthetic is clean and modern.

FROST: Forest of Scintillating Glass Tubes

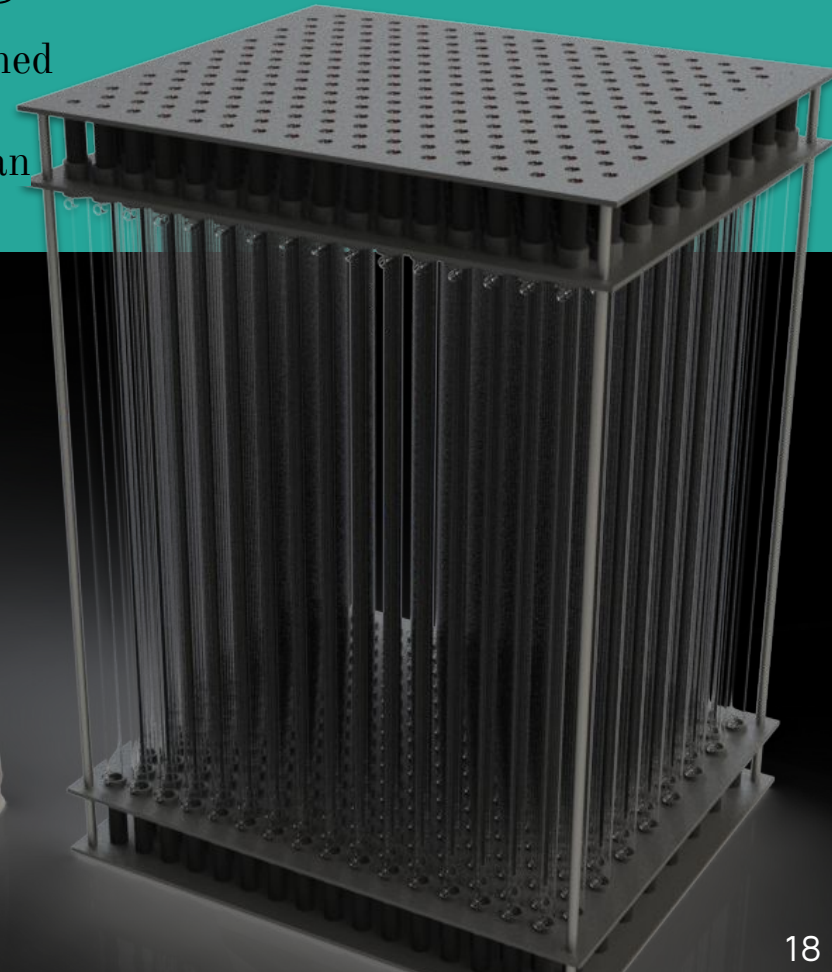
Max Asa Albert Dornfest
Fourth year Physics Ph.D. student
Email: Dornfest@Hawaii.edu

PI: Dr. John Learned
Working with:
Viacheslav Li, Brian
Crow, Gabe Yopez

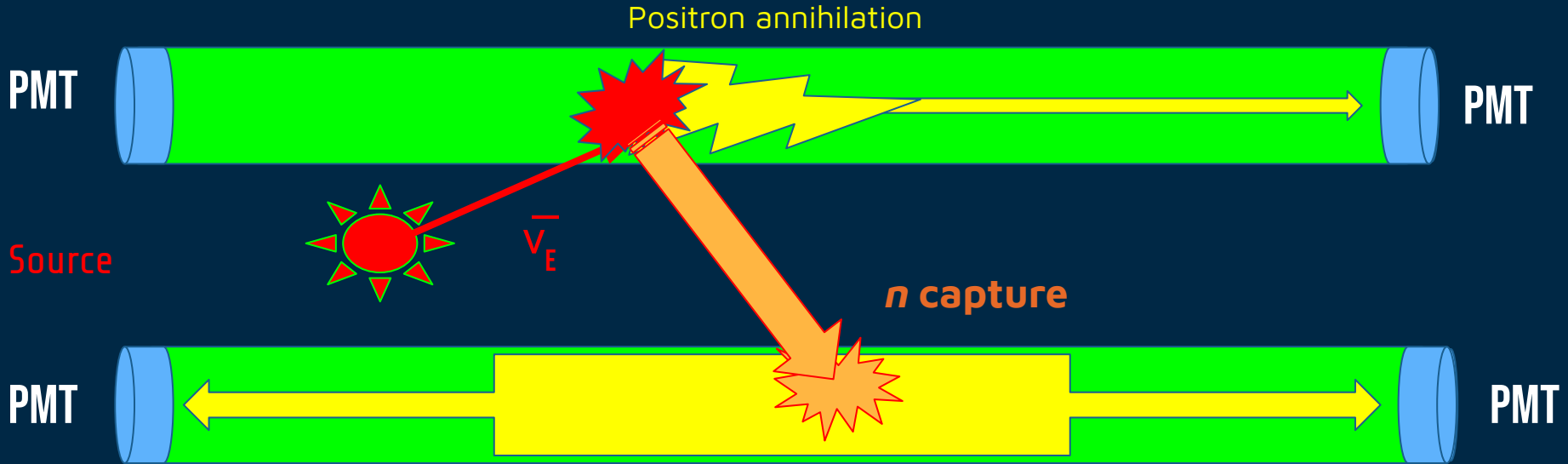
Purpose: Observing nuclear reactors from afar for **nuclear non-proliferation**

Principle of operation: Observe anti neutrino interaction in one tube and outgoing neutron direction and energy from another tube in the forest.

FROST-TEA: Thousands of modular vertical quartz tubes $\sim 3\text{cm}$ diameter filled with organic scintillator and PMTs at the ends.



Subsequent New Design - *FROST* - Diagram



FROST - Laboratory Setup

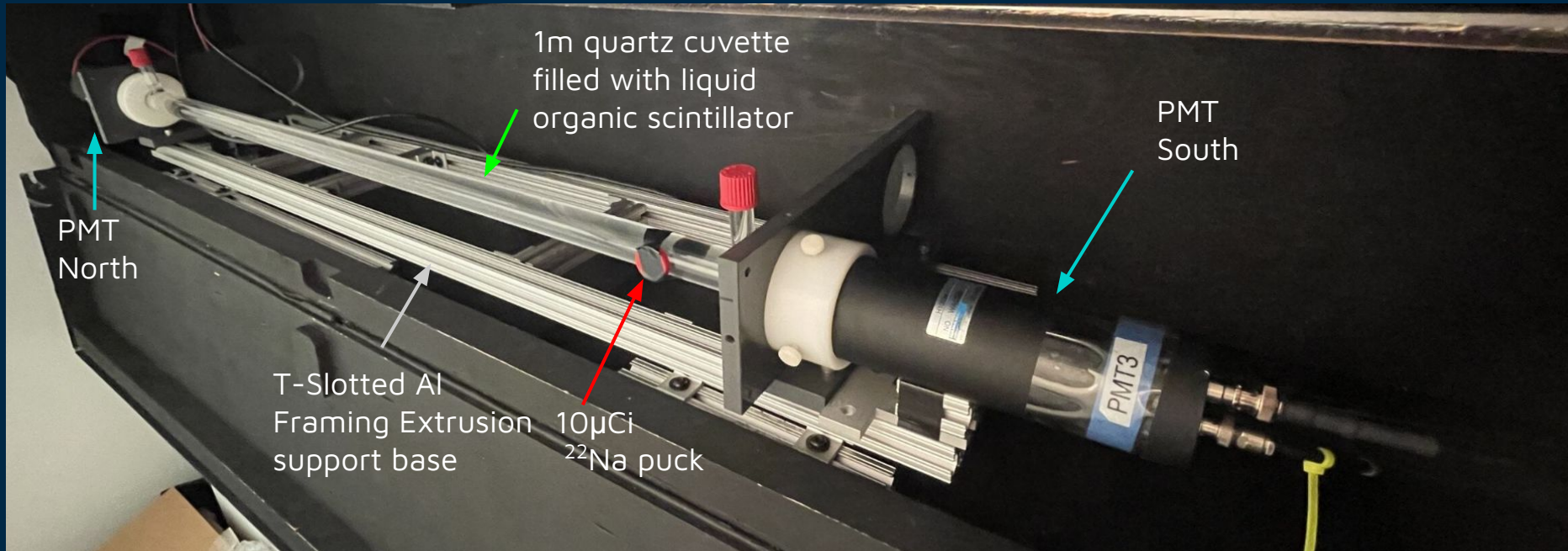


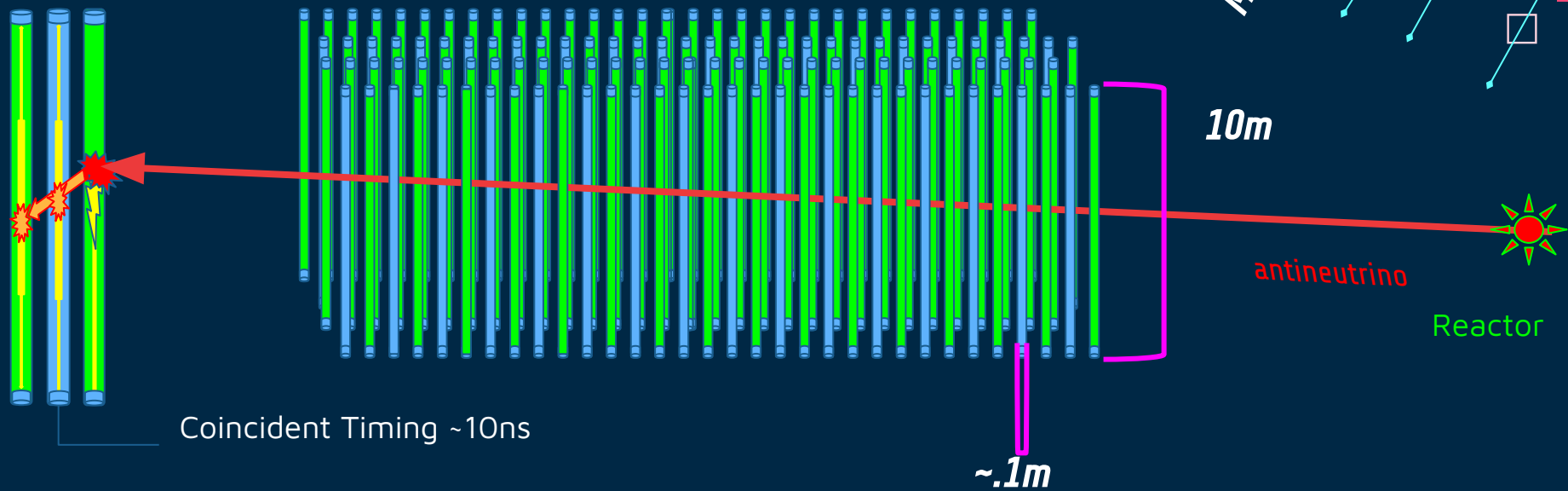
Fig. (above): FROST setup with ^{22}Na gamma puck for experimental verification of light yield and energy resolution.

Final Design - *FROST-TEA* (Theoretical End Arrangement)



Figure: To scale SolidWorks CAD overlaid with map showing 13km between Morton mine and Perry NPS. An illustrative deployment scenario; was proposed by WATCHMAN: A WAter CHerenkov Monitor for ANtineutrinos

Final Design - *FROST-TEA* (Theoretical End Arrangement)



Coincident Timing $\sim 10\text{ns}$

Figure illustrating the "forest" in FROST.

Note the green cuvettes are filled with scintillator and the blue ones are not.

Final Design – *FROST-TEA* (Theoretical End Arrangement)

MUONS

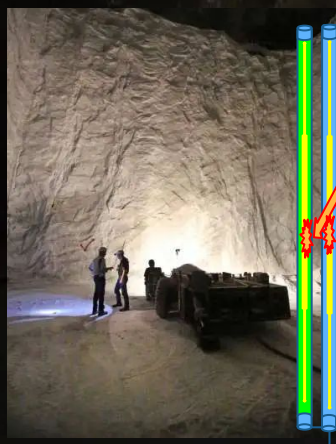
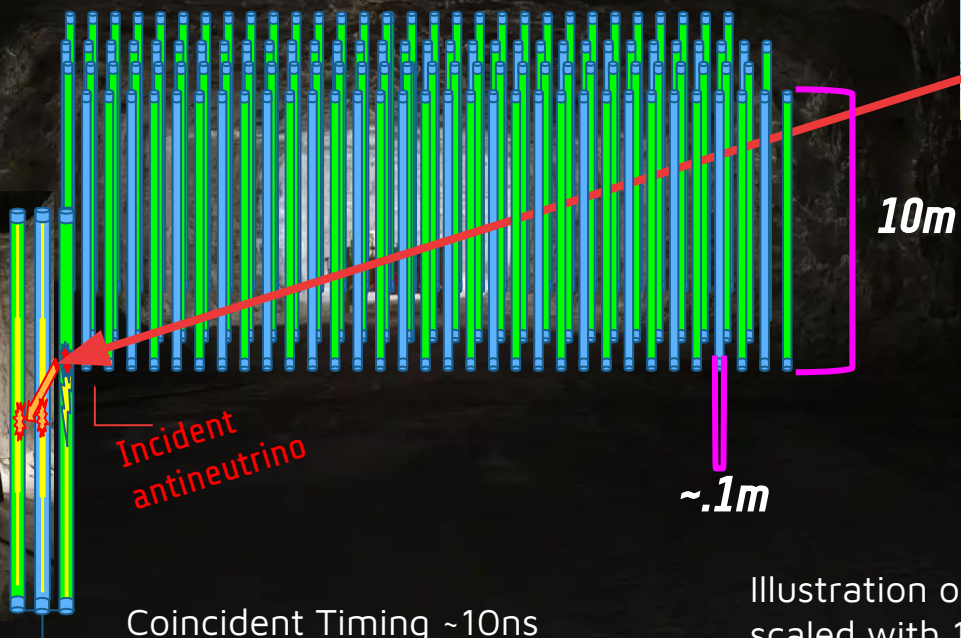


Illustration of FROST-TEA with 10m trees scaled with 1.6m tall humans.

Future and Ongoing Work – Small Modular Reactor Simulations

Following Double Chooz's formulation (same as our paper and this presentation). Using our work on NuLat

$$[\Delta\varphi]_{1\sigma} = \arctan\left(\frac{P/d}{\sqrt{N}}\right) \quad (1) \quad N_{\nu_e} = \frac{1}{4}n_H V \sigma \frac{dN_{\nu_e}}{dt} \frac{1}{4\pi L^2} t \quad (2)$$

Where the factor of 1/4 corresponds to proportion of $\bar{\nu}_e$ above IBD threshold, V is the volume, σ is the cross section for IBD events, L is distance to source, and n_H is a normalization function for target mass.

We would like to find the relationship of detected events N, to directionality and so we want to find $\frac{\partial N_{\bar{\nu}_e}}{\partial \varphi}$

An easier method would be solving for N and writing out $\frac{\partial[\Delta\varphi]_{1\sigma}}{\partial N}$

Naively, using (1)&(2) and treating P and d as constants, then $\frac{\partial}{\partial N} \arctan\left(\frac{P/d}{\sqrt{N}}\right) = \frac{-d \times P}{2\sqrt{N}(d^2N + P^2)} \quad (3)$

Max's Model - dummy variable or one-hot encoding.

$$N(L, \varphi)_i = \sum_{i=1, j=0,1}^{detectors} (f(L) + g(\varphi)\delta_j)_i \quad (4)$$

Where f and g are general functions for mono-detector and angular efficiency (respectively), and δ_j is an indicator function for one-hot encoding:

$$\delta_j \begin{cases} 1 & \text{if } j = 1, \\ 0 & \text{if } j = 0. \end{cases} \quad (5)$$

Note: As with any addition of variables to a model, the addition of dummy variables increases the within-sample model fit (coefficient R²), but at a cost of fewer degrees of freedom and loss of generality of the model (out of sample model fit).

Summary and Conclusion

- Shown how a variety of small existing and hypothetical inverse beta decay detectors can measure the incoming direction of electron-antineutrinos, given a sufficient number of events.
- Furthermore, our publication studied how detector design shows promise for improving the angular resolution of these measurements within reasonable timescales for our targeted near-surface, low-standoff deployment scenario.
- Combining finding the directionality and range one may achieve **blind recognition** of a reactor's existence, azimuth, distance and power, with mature existing technology.

“While not an easy task, it is a remarkable capability unique to neutrinos — the only stable elementary particles which “know” their point of origin!”

- John Learned

Acknowledgements and Credits

Material, unless otherwise cited, was taken from Mark Duvall's Directionality Paper, my FROST work, and our corresponding Physical Review Applied publication <https://arxiv.org/abs/2402.01636> (sans logos below).

Thank you to the Consortium for Monitoring, Technology, and Verification (MTV) for support and funding.

Thank you to RWTH, Rheinisch-Westfälischen Technischen Hochschule Aachen, and local organizers Yan-Jie Schnellbach and Stefan Roth.

Finally, thank you to you, my audience.



University of Hawai'i at Mānoa

Department of Physics & Astronomy

Backup Slides - Sensitivity

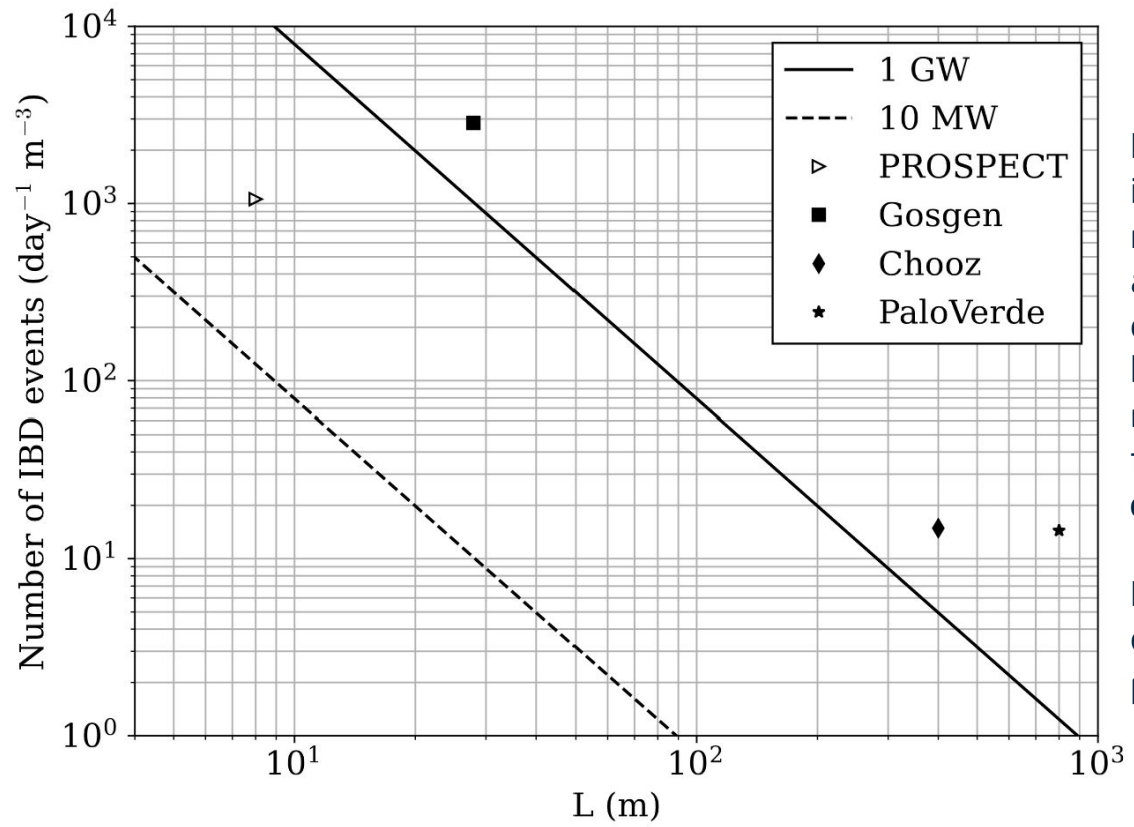


Fig. (left): Number of IBD interactions per day per cubic meter of detector volume, using a detector medium with 5×10^{22} cm⁻³ number density for hydrogen. Various power and research reactors cited above are featured as test points for **directionality**.

Note that upwards on the plot is equivalent to increasing reactor power.

Backup Slides - Simulated NuLat 3³ Geometry

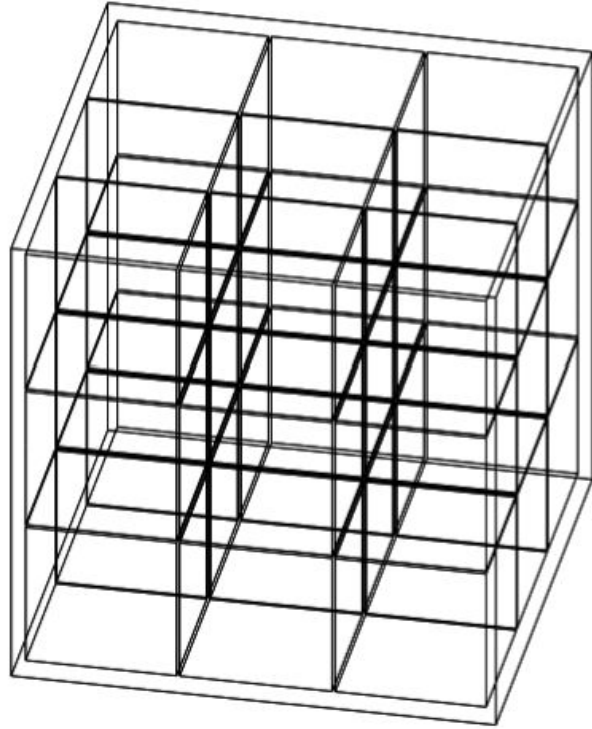


Fig. (left): a 3x3x3 array of ⁶Li-doped scintillator cubes. The cubes have a 5-cm side length and are separated by a 1-mm air gap.

For this arrangement, the IBD interaction vertices (and therefore the prompt events) are restricted to the central cube only; but the delayed events can occur in any of the 27 cubes.

Backup Slides - SANTA Design Concept

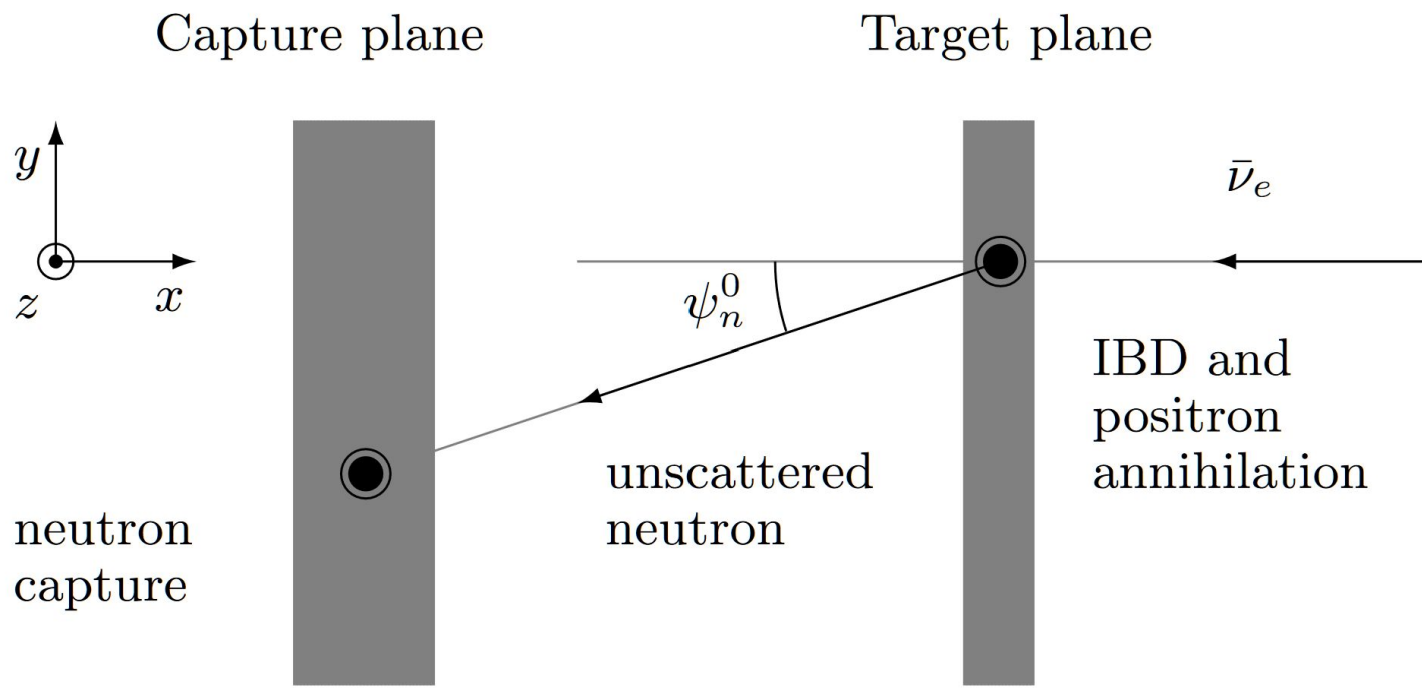


Fig. (above): Design concept of a target-capture-plane detector based on the SANTA. In this study, the antineutrino direction was perpendicular to the detector planes. Only one capture plane was implemented (unlike the original design with the second capture plane). Angle ψ_n^0 is the angle between the direction of capture-IBD cells and the x -axis. In the separation detector like SANTA, the mean values for angles ψ_n^0 and φ are the same. [arXiv:2402.01636](https://arxiv.org/abs/2402.01636)



Backup Slides – Simulated SANTA Geometry

Both planes:
40 bars \times 5 cm tall

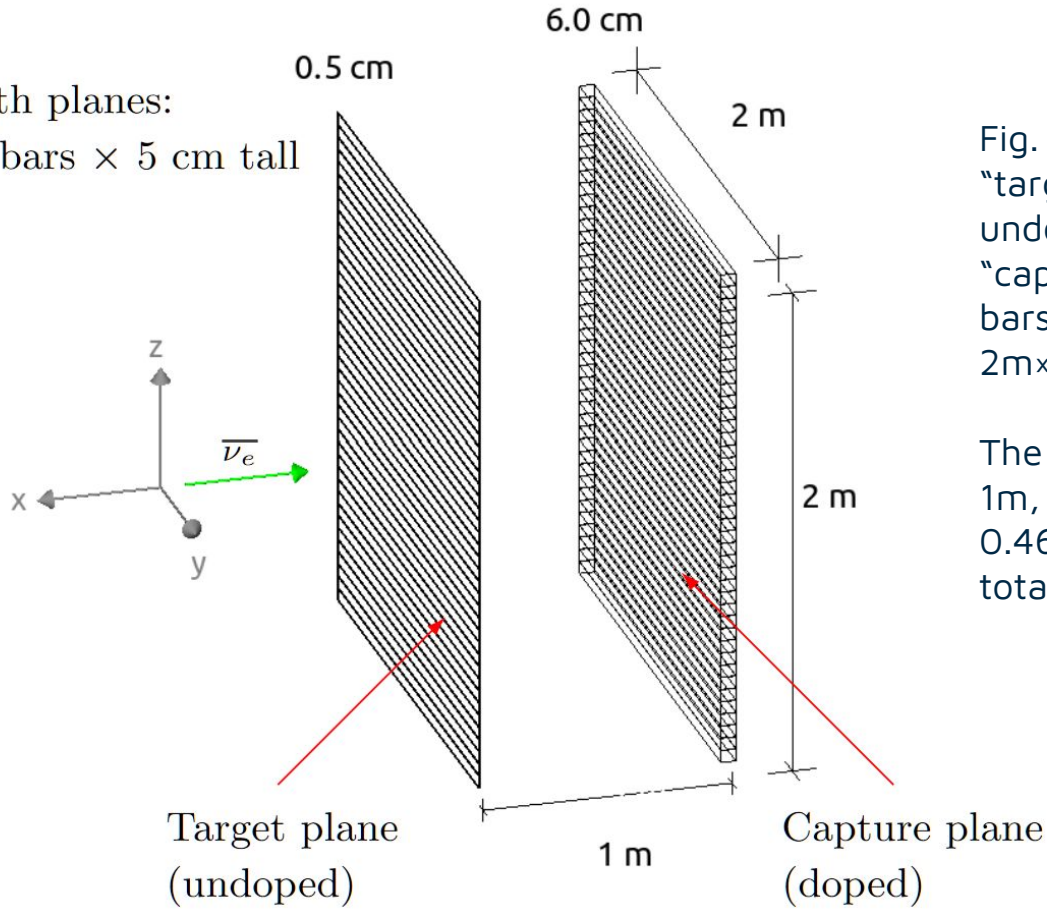


Fig. (left) Simulated SANTA Geometry — the “target” plane comprised of 40 bars of undoped scintillator 2m \times 0.05m \times 0.005m; the “capture” plane comprised of 40 scintillator bars doped with natural boron, 2m \times 0.05m \times 0.06 m.

The separation between the two planes is 1m, resulting in a “packing factor” of about 0.46% (the ratio of the target volume to the total volume of the detector).

Backup Slides - Checkerboard 3D Geometry

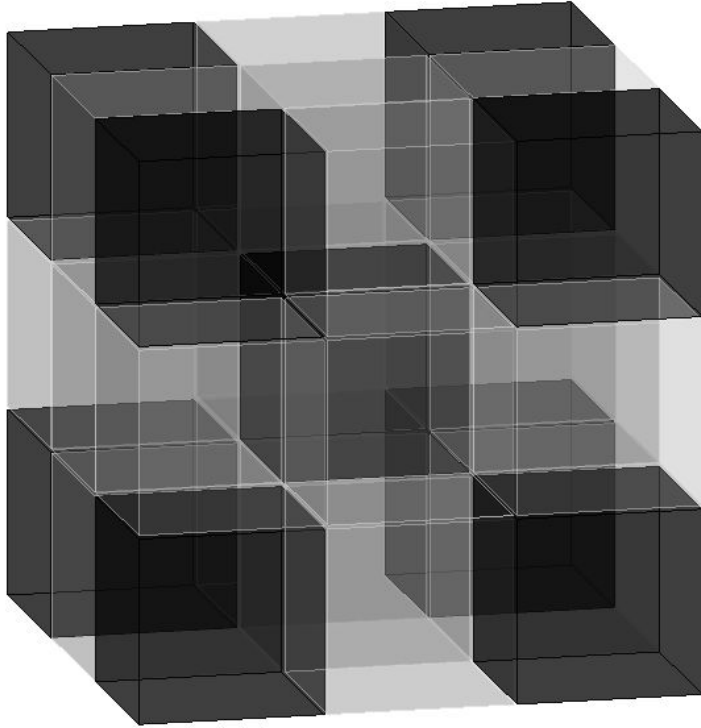


Fig. (left): Closeup showing a $3 \times 3 \times 3$ arrangement for 3D "checkerboard" lattice (inert cells ghosted).



Backup Slides - Results - Neutron Scattering

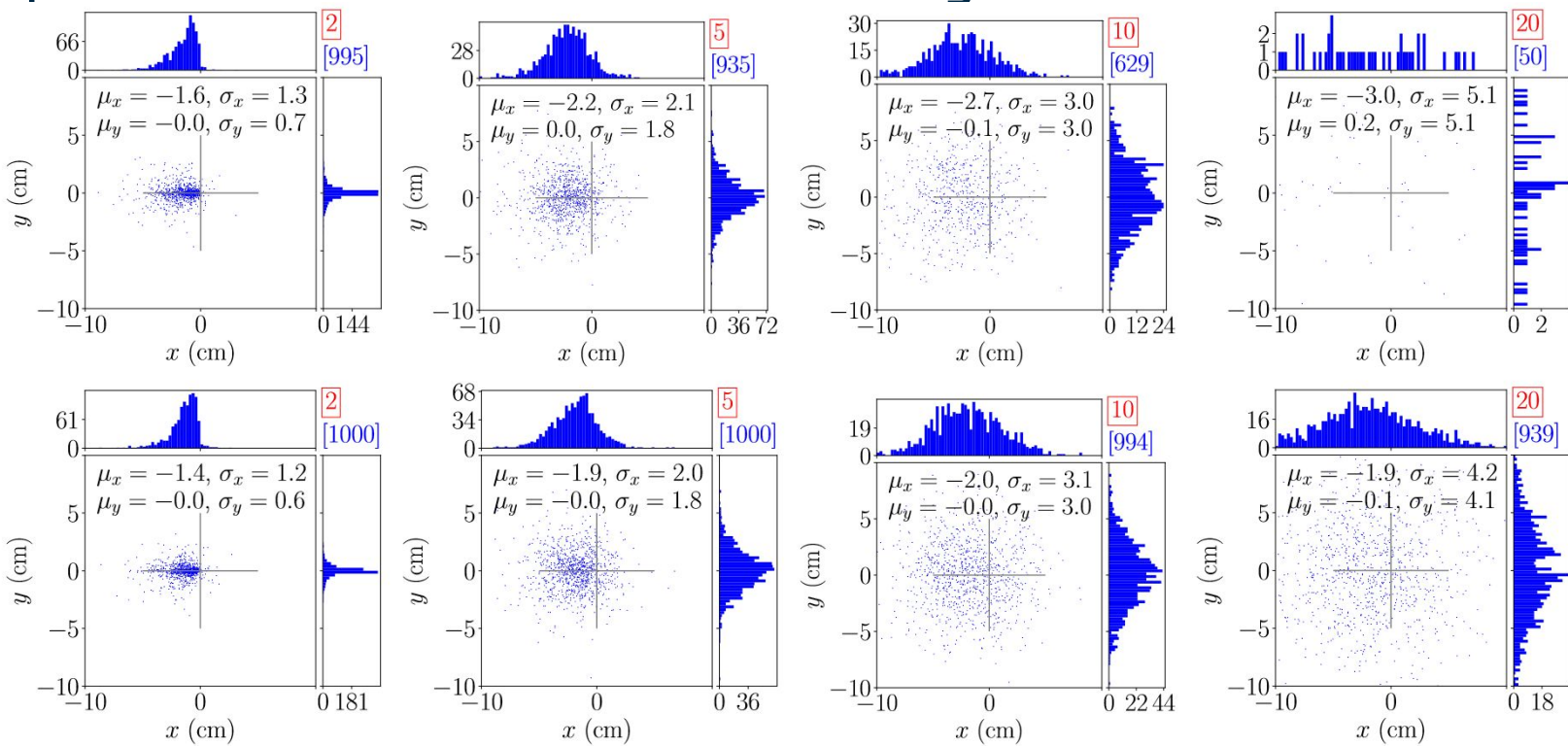


Fig. above: Displacements at 2nd, 5th, 10th, and 20th scatterings for 4keV neutrons along $\{-1,0,0\}$ inside a large volume of plastic scintillator; (top row) doped at 1.5wt% ${}^6\text{Li}$, (bottom row) undoped.

For the undoped scintillator, the neutrons undergo a higher number of scatters on average, making the displacement more obvious. Displacements in xy-plane; the gray cross (10-cm across) indicates the origin and the scale to make the displacement in the distributions more visible.

Backup Slides - Results - Distribution of $\cos\psi$ - Doped and Undoped

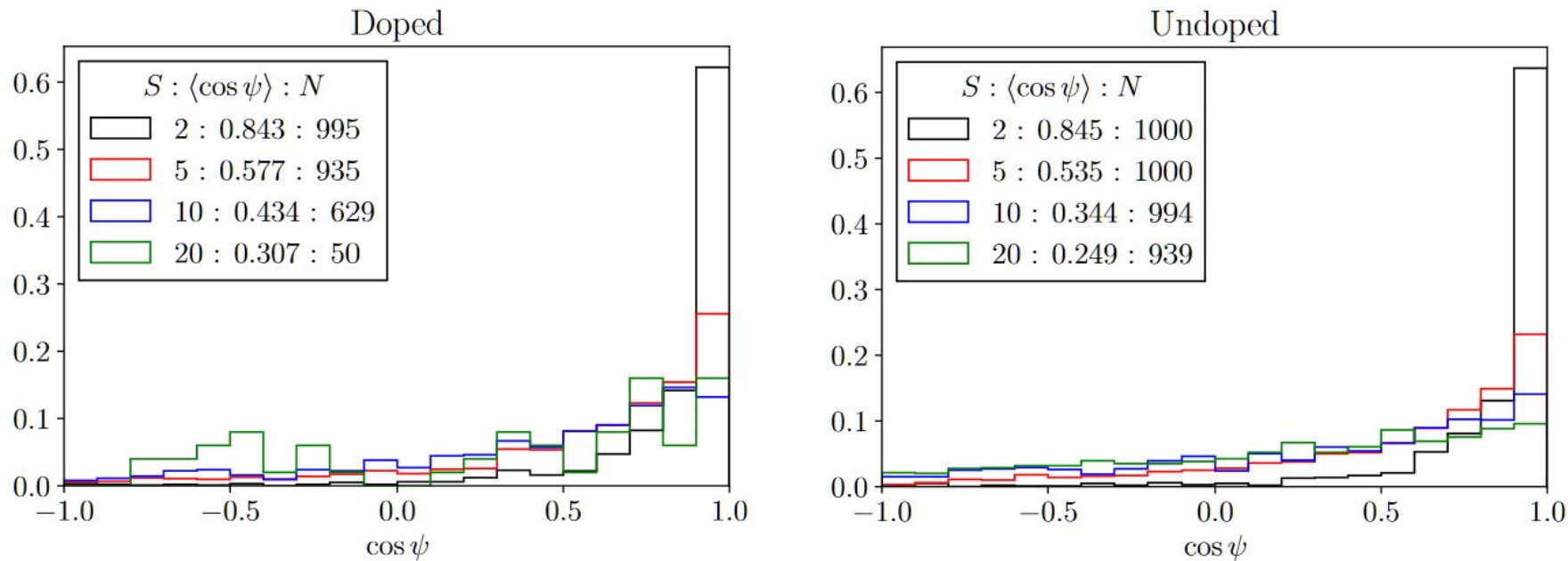


Fig. (above): Distribution of the $\cos\psi$ for various number of scatters (indicated in the legend along the mean values). The mean values indicate the strength of the directional trend. Number of neutrons left after S number of scatters is indicated in the legend, i.e. the number of entries in the corresponding histogram.

Backup Slides - Results - Normalized Distribution of $\cos\psi$ - 2D and 3D

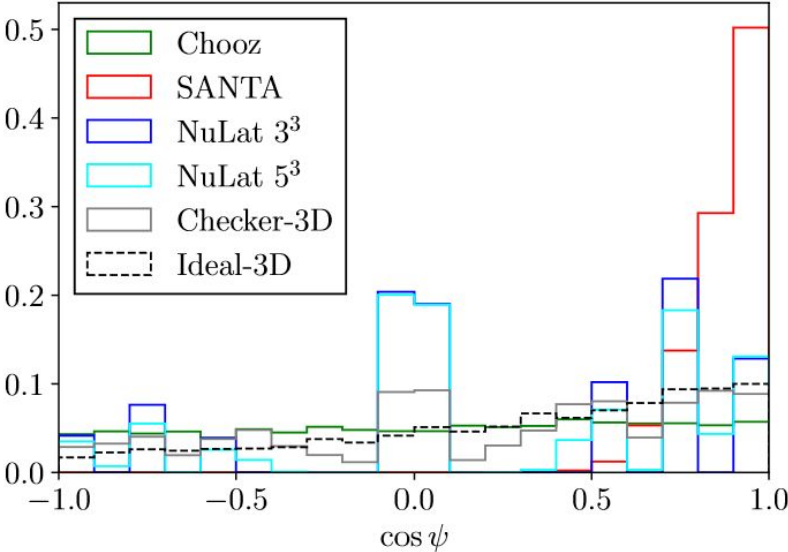
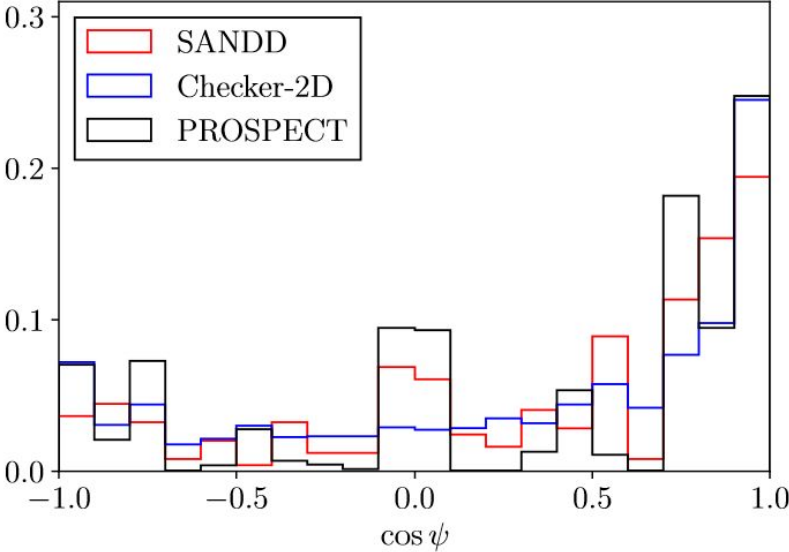


Fig. (above): Normalized distribution of $\cos\psi$ for 2D (left) and 3D (right). The Chooz-like monolithic detector is listed among the 3D detectors. The “Ideal- 3D” distribution indicates the simulated directional performance of a 1.5%-wt. ⁶Li-loaded, monolithic detector with a hypothetical perfect position resolution (i.e., $\delta\{x,y,z\} \equiv 0$). It effectively represents the theoretical maximum directional performance of a non-segmented detector (with this particular target material), due to the neutron-scattering problem.

Results Table

Recon. Type	Experiment	Dopant	%wt.	Vol. (L)	P (mm)	d (mm)	N_{trg}	N_{1V}	N	$\langle \cos \psi \rangle$	φ (°)	$\Delta\varphi$ (°)
3D	DC (data)	Gd	0.1	10 000	156.7	16.7	8249	—	8249	0.059	7.4	5.90
	Monolithic	Gd	0.1	785 000	125.27	13.9	9198	—	9198	0.052	-2.55	5.37
	NuLat 5 ³	⁶ Li	1.5	15.6	43.4	20.0	4592	661	3931	0.256	0.82	1.98
	3D Chkbd.	⁶ Li	1.5	107.	105.7	32.7	4384	178	4206	0.194	6.03	2.85
	SANTA	B	0/5	24.0	218.28	1000.0	2275	0	2275	0.876	-0.56	0.26
2D	SANDD-CM	⁶ Li	1.5	0.64	16.8	10.0	250	3	247	0.360	12.08	6.10
	2D Chkbd.	⁶ Li	1.5	5.12	55.6	24.8	1864	4	1860	0.297	4.02	2.98
	PROSPECT	⁶ Li	0.08	3 465	150.07	36.8	9489	239	3726	0.335	3.03	3.82

TABLE: Summary of results.

The total number of IBDs simulated in each detector is 10 000. Target material is PVT for all detectors except for DoubleChooz. N_{trg} is the total number of IBD-candidate events registered by the antineutrino trigger. N_{1V} is the number of IBD-candidate events for which the prompt and delayed events occurred within a single volume/segment; these events were not used for directional reconstruction except in the monolithic (Chooz-type) detector. $N = N_{trg} - N_{1V}$ is the resulting number of IBD-candidate events used for directional reconstruction. $\langle \cos \psi \rangle$ is a measure of angular accuracy, and $\Delta\varphi$ is the 1σ angular uncertainty on the reconstructed direction to the antineutrino source; it is the half-aperture of a cone in the 3D experiments and the half-angle of an arc in the 2D experiments. Note that the 2D experiments are reconstructing the *azimuthal angle only*.